Available online at www.sciencedirect.com
ScienceDirect
Catalysis Today 130 (2008) 170–177
CATALYSIS TODAY
www.elsevier.com/locate/cattod

A density functional theory study of the hydrodesulfurization reaction of dibenzothiophene to biphenyl on a single-layer NiMoS cluster

Thomas Weber [a,*], J.A. Rob van Veen [b]

[a] *Institute for Chemical and Bioengineering, Swiss Federal Institute of Technology (ETH), Wolfgang-Pauli-Strasse 10, HCI E 117, CH-8093 Zurich, Switzerland*
[b] *Shell Research and Technology Centre, 1030 BN Amsterdam, The Netherlands*

Available online 9 August 2007

Abstract

The hydrodesulfurization of dibenzothiophene on a NiMoS cluster consisting of 1 Ni and 18 Mo atoms was investigated by means of density functional theory. The calculations focus on the direct desulfurization pathway where dibenzothiophene reacts with H_2 to biphenyl and H_2S. Critical steps with high activation energies are breaking of the two C–S bonds of the DBT molecule (ca. 32 kcal/mol), the activation of H_2 by heterolytic dissociation and the removal of the formed biphenyl molecule from the catalyst surface (17 kcal/mol, respectively). All other reaction steps have activation energies of $\leq$10 kcal/mol.

Keywords: Density functional theory; Hydrodesulfurization; H_2 dissociation; C–S bond breaking; Sulfide catalysis; Nickel–molybdenum sulfides

1. Introduction

Catalytic hydrodesulfurization (HDS) consists in the removal of sulfur from crude oil at temperatures around 300 °C and medium–high pressures of H_2 gas in the presence of a transition-metal sulfide catalyst. Under these reaction conditions sulfur-containing organic molecules present in the feed decompose to hydrocarbons and H_2S. The most widely used catalysts contain MoS_2 phases promoted with cobalt or nickel [1,2]. Organosulfur compounds found in crude oil differ in structure and size, and thus in reactivity towards H_2. Dibenzothiophene and its alkyl-substituted derivatives belong to the most difficult compounds to desulfurize. For these compounds two basic HDS reactions have been identified as being responsible for the removal of sulfur: direct desulfurization (DDS) and hydrogenation (HYD) followed by sulfur removal.

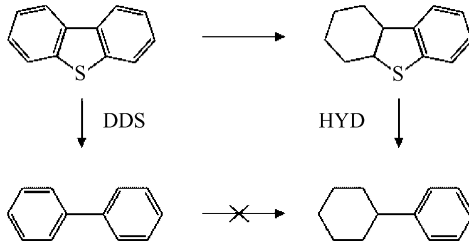

(1)

In the direct desulfurization reaction, which is the main route, dibenzothiophene and H_2 react to biphenyl and H_2S. The hydrogenation reaction involves the hydrogenation of one of the benzene rings of dibenzothiophene, followed by desulfurization of the resulting hexahydrodibenzothiophene to yield cyclohexylbenzene. A large body of theoretical research has aimed at understanding the mechanisms of C–S bond breaking of thiophene and dibenzothiophene through their interaction with the metal sulfide catalyst surfaces [3–14]. In spite of the intensive research into HDS, the mechanism of the direct desulfurization of dibenzothiophene, is still being disputed. One mechanism under discussion assumes a hydrogenolysis reaction, during

* Corresponding author. Tel.: +41 44 632 3043; fax: +41 44 632 1162.
E-mail address: thomas.weber@chem.ethz.ch (Th. Weber).

0920-5861/$ – see front matter © 2007 Elsevier B.V. All rights reserved.
doi:10.1016/j.cattod.2007.06.078

which C–S bonds are broken under simultaneous formation of C–H and S–H bonds. In this case biphenyl would directly form on the catalyst surface from dibenzothiophene and hydrogen [1,2,15,16]. A related mechanism may be the insertion of a metal atom in the C–S bond, followed by hydrogenation, as observed in organometallic complexes of thiophene and benzothiophene [17–20]. This, however, is unlikely in the case of the heterogeneous reaction, because of the rigidity of the catalyst structure. Others argue that the mechanism consists of hydrogenation of dibenzothiophene to dihydrodibenzothiophene, followed by elimination to give biphenyl and H_2S [21]. The much simpler hydrogenolysis reaction of alkanethiols to alkanes has not been studied in depth either, and only very few experimental data are available. This reaction is complicated by the occurrence of the parallel elimination reaction of the alkanethiols to alkenes. Over metal sulfide catalysts the HDS of alkanethiols is already fast at 500 K [22]. In a recent theoretical work the kinetic properties of the hydrogenolysis and elimination reactions of alkanethiols could be described satisfactorily. Todorova et al. studied by means of density functional theory (DFT) calculations the adsorption, dissociation, and reaction of methanethiol [23] and ethanethiol [24] on the catalytically active Mo edge of MoS_2 as a function of the sulfur coverage and presence of hydrogen and promoter atoms. These molecules were chosen to investigate the hydrogenolysis reaction, i.e., C–S bond scission, and the parallel elimination pathway independently. Whereas methanethiol can only react to methane via hydrogenolysis, ethanethiol possesses a β-hydrogen atom and can undergo elimination to ethene and H_2S in addition to hydrogenolysis to ethane. The authors found that after molecular adsorption on the (1 0 0) MoS_2 surface, C_2H_5SH showed slightly lower energy barriers for desorption of the reaction products than CH_3SH. The C_2H_6 formation and desorption from ethanethiolate proceed with a lower energy barrier than the C_2H_4 formation and desorption from the molecularly adsorbed C_2H_5SH state.

These results provide a better understanding of mechanisms, which occur in the more complex reactions of larger sulfur-containing molecules and form the basis of our DFT calculations of the desulfurization of dibenzothiophene. We performed calculations of the dibenzothiophene HDS reaction over promoted and unpromoted MoS_2 particles by using periodic surface structures and small clusters as catalyst particles. While the results obtained with periodic surface structures will be published elsewhere, this paper presents the computational results of the direct desulfurization pathway of the hydrodesulfurization reaction of dibenzothiophene to biphenyl on a Ni-promoted single-layer MoS_2 cluster.

2. Computational details

The computational method that we used in the DFT calculations is based on those described in [23,24] but with slight modifications to adapt to the systems calculated here. We used the DMol^3 code [25] (Materials Studio 4.0 and 4.1, Accelrys) with a double-numeric polarized basis set, a medium level of integration grid consisting of approximately 1000 grid points per atom, and DFT semi-core pseudopotentials for the core-treatment. The nonlocal exchange-correlation functional of Perdew and Wang (PW91) was applied [26]. These settings allow for calculating energies with an accuracy of ±0.1 kcal/mol. The following geometry optimization convergence thresholds were used: 0.01 kcal/mol (energy change), 2.5 kcal/(mol Å) (maximum force) and 0.005 Å (maximum displacement). Spin states were explicitly set.

The NiMoS cluster was created as illustrated in Fig. 1. We started with the generation of bulk 2H–MoS_2 from published

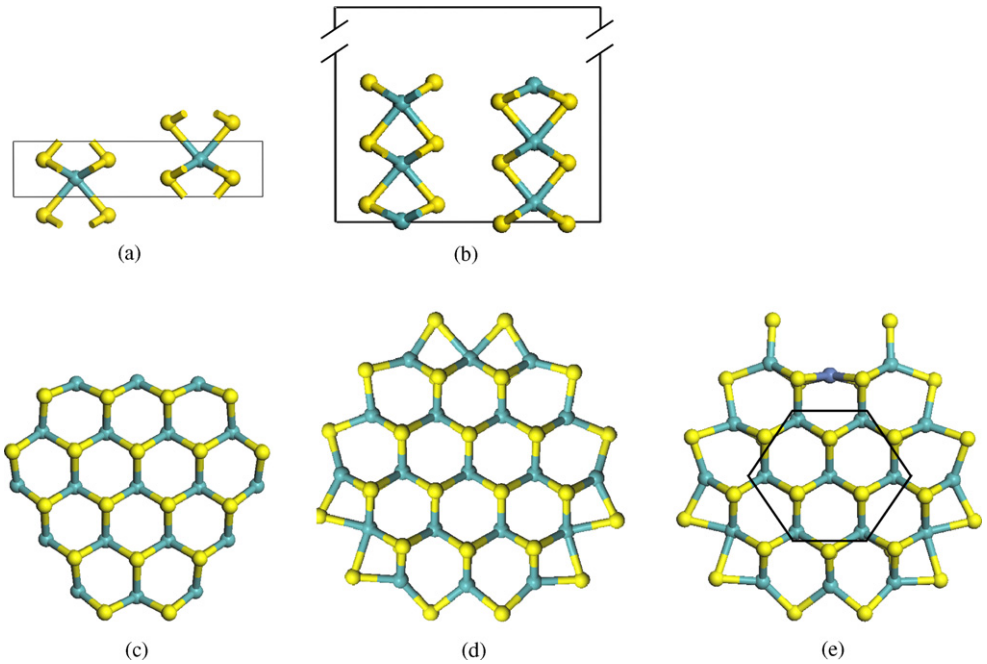

Fig. 1. Construction of the single-layer NiMoS cluster. (a) Bulk structure of 2H–MoS_2; (b) (1 0 0) surface of 2H–MoS_2; (c) MoS_2 particle extracted from structure (b); (d) MoS_2 cluster with optimized edge sulfur coverage; (e) NiMoS cluster. The hexagon indicates the constrained central Mo_7S_6 fragment.

X-ray data [27] and subsequent optimization of the unit cell (Fig. 1a). Next we generated the (1 0 0) surface of 2H–MoS_2 and performed a full structural optimization (Fig. 1b). The periodic surface structure was decomposed and a single-layer MoS_2 particle consisting of 19 Mo atoms was extracted, optimized (Fig. 1c) and the surface sulfur atoms were reorganized so that an average 50% occupation of the metal and the sulfur edges was reached (Fig. 1d). The rearrangement of the sulfur atoms leads to an energy gain of 247 kcal/mol. Finally a molybdenum atom of the metal edge was replaced by nickel, the resulting cluster was optimized (Fig. 1e) and a central Mo_7S_6 fragment of the particle was stabilized by applying geometry constrains.

To calculate the minimum energy path between several reaction steps we used the linear/quadratic synchronous transit (LST/QST) method [28] proposed by Halgren and Lipscomb [29] and implemented in the DMol^3 code [25]. The activation energy is determined by the highest maximum on the minimum energy path, obtained by the LST/QST method. The reaction path was divided into several steps between the respective reactant and products by interpolating along the path segments following the adiabatic valley of the potential surface. We calculated the energies of these steps, as well as the adsorption barriers. The success of the calculations with the LST/QST method is based on the close proximity of the end points for the transition state search. The refinement of the transition state has been done by optimizing the transition state following the eigenvector of the Hessian matrix corresponding to the imaginary frequency mode. It has thus been verified that the transition states have only one imaginary frequency. The calculations of the dissociation of H_2 on (1 0 0) 2H–MoS_2 surfaces in Ref. [30] present a more detailed description of how the LST/QST method is used for DFT transition-state calculations.

3. Results and discussion

Hydrodesulfurization of dibenzothiophene occurs according to two different types of reaction, namely direct desulfurization (DDS) and hydrogenation (HYD) as illustrated in scheme (1). Direct desulfurization is the main route in this network and therefore, the focus of our interest. In DDS, dibenzothiophene (DBT) reacts on the catalyst surface with H_2 to biphenyl (BP) and H_2S. During this process H–H and C–S bonds are broken, while C–H bonds are formed. Breaking the H–H bond of the H_2 molecule is much easier than splitting the C–S bonds of the DBT molecule. For this reason we assume that the surface of the catalyst particle is sufficiently covered with hydrogen when the DBT molecule adsorbs. Therefore, one catalytic cycle of the DDS reaction can be divided into three parts: (I) the activation of H_2 on the catalyst surface, (II) the adsorption and reaction of DBT with subsequent desorption of the formed BP and, finally, (III) cleavage of the catalytic site with H_2. We calculated a mechanism that consists of several individual steps (see Fig. 2) where all processes occur at, or at least in close vicinity of the Ni promoter atom.

In our mechanism the catalytic cycle starts with one DBT and two H_2 molecules in the gas phase above the catalyst particle at a non-interacting distance (Fig. 2, state 1) and ends accordingly with the products BP and H_2S (Fig. 2, state 10). Activation of hydrogen consists in transferring of one H_2 molecule from the gas phase to a stable equilibrium distance close to the active site of the catalyst surface (Fig. 2, 1 → 2) and subsequent heterogeneous splitting, yielding S–H and Ni–H surface species (Fig. 2, 2 → 3). The next steps deal with the desulfurization of DBT and formation of BP. The DBT molecule moves from the gas phase to a stable equilibrium state above the Ni atom of the catalyst particle (Fig. 2, 3 → 4), adsorbs under breaking of one C–S bond (Fig. 2, 4 → 5) and

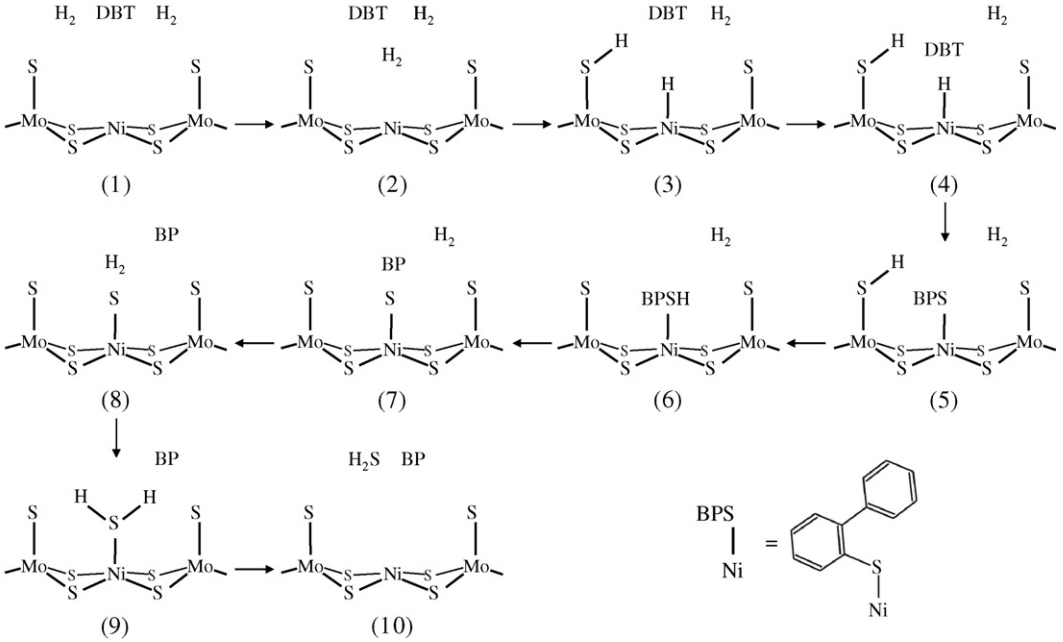

Fig. 2. Calculated mechanism of the DDS pathway of the dibenzothiophene HDS reaction (DBT: dibenzothiophene, BP: biphenyl).

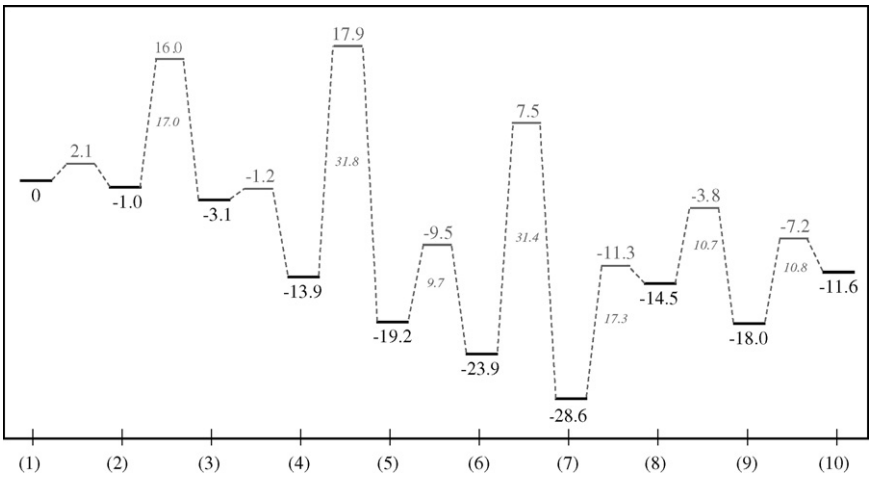

Fig. 3. Energy profile of the DDS pathway of the dibenzothiophene HDS reaction reaction. States 1–10 refer to reaction steps in Fig. 2. Energy values are in kcal/mol and referenced to state 1, which was arbitrarily set to zero. For steps with activation energies of about 10 kcal/mol or more, absolute activation energies are given in italics.

reacts to an BPSH intermediate via H-transfer from the catalyst SH surface group to the sulfur atom of the organic molecule (Fig. 2, 5 → 6). Next the product BP forms in a concerted mechanism in which the sulfur and the hydrogen atoms of the BPSH intermediate change their positions (Fig. 2, 6 → 7) and desorbs from the catalyst surface (Fig. 2, 7 → 8). The last steps of our mechanism deal with the cleavage of the catalytic site, i.e., removal of the sulfur ligand from the Ni centre. This proceeds via reaction with the remaining H_2 molecule. The H_2 molecule converts the Ni–S surface species into a Ni–SH_2 group (Fig. 2, 8 → 9), from which H_2S is released into the gas phase (Fig. 2, 9 → 10).

The calculated energy profile of this reaction sequence is shown in Fig. 3. All energy values are referenced to state 1, which is arbitrarily set to zero. The energy profile shows that the overall reaction (1 → 10) is exothermic by −11.6 kcal/mol, which is in good agreement with our calculated value of the non-catalyzed gas-phase desulfurization reaction of DBT (−12.2 kcal/mol). Most of the single reaction steps are exothermic with moderate activation energies ≤10 kcal/mol. Four steps, however, show significantly higher activation energies. These are key steps in our mechanism and consist in the splitting of the H_2 molecule (2 → 3, 17.0 kcal/mol), the Ni–DBT complex formation under C–S bond breaking (4 → 5, 31.8 kcal/mol), the formation of BP from the BPSH intermediate (6 → 7, 31.4 kcal/mol) and the release of the BP molecule from the catalyst surface (7 → 8, 17.1 kcal/mol).

3.1. Activation of H_2 on the catalyst surface

The activation of dihydrogen gas proceeds in two steps, i.e., the adsorption of H_2 from the gas phase on the catalyst surface and its subsequent heterolytic splitting into S–H and Ni–H species. The adsorption process (Fig. 2, 1 → 2) is slightly exothermic (−1.0 kcal/mol), and has a very low activation barrier (2.1 kcal/mol), because it is the translational motion of the H_2 molecule and some minor relaxation of the cluster surface. Whereas the adsorption is a physical process, the dissociation of H_2 (Fig. 2, 2 → 3) is clearly a chemical reaction. In the initial state (Fig. 4, structure a) the H_2 molecule is symmetrically located above the Ni promoter atom at a distance of d(Ni–H) = 1.85 Å. Although this distance is too long for considering it an Ni–H bond (the length of a covalent Ni–H bond should be d_{cov}(Ni–H) = r_{cov}(Ni) + r_{cov}(H) = 1.15 + 0.3 = 1.45 Å), there is clearly an attractive interaction between the H_2 molecule and the catalyst particle as evidenced by changes in the H–H distance and the local environment of the nickel atom. In the isolated cluster (Fig. 1e), the Ni centre is located at a position below that of the Mo atoms, leading to an Mo–Ni–Mo angle of 159.2° (in the case of an unpromoted surface the respective Mo–Mo–Mo angle is ≈180°). Upon adsorption the Ni centre is slightly pulled to the surface (∠Mo–Ni–Mo = 167.7°) and the H–H distance increases (d(H–H) = 0.76 Å versus 0.73 Å in the free molecule), which points to a weak activation of the H_2 molecule. The heterolytic splitting of H_2 on this cluster is exothermic by −2.1 kcal/mol and goes along with a moderate activation energy of 17.0 kcal/mol, which is in good agreement with the results of Todorova et al. [30] and Sun et al. [31] for the respective reaction on periodic (1 0 0) MoS_2 surfaces. In both references a discussion of other published data, such as that of Refs. [10–12], can be found. In the final state (Fig. 4, structure c) hydrogen is clearly dissociated (d(H–H) = 2.64 Å) and is present in the form of a ''proton'' (SH group, d(S–H) = 1.34 Å) and a hydride species (Ni–H fragment, d(Ni–H) = 1.44 Å). The Ni centre slightly moved back into the structure towards its original position (∠Mo–Ni–Mo = 165.4°) and the geometry of the two Mo–S surface species adjacent to the Ni centre has changed. In the isolated cluster both Mo–S bonds are equal (d(Mo–S) = 2.13 Å, ∠S–Mo–Ni = 97.7°), whereas after dissociation of H_2, the symmetry of the cluster surface has lowered: d(Mo–S_1) = 2.35 Å, ∠S_1–Mo–Ni = 104.5°, d(Mo–S_2) = 2.13 Å, ∠S_2–Mo–Ni = 101.8°. Relevant structural parameters are listed in Table 1.

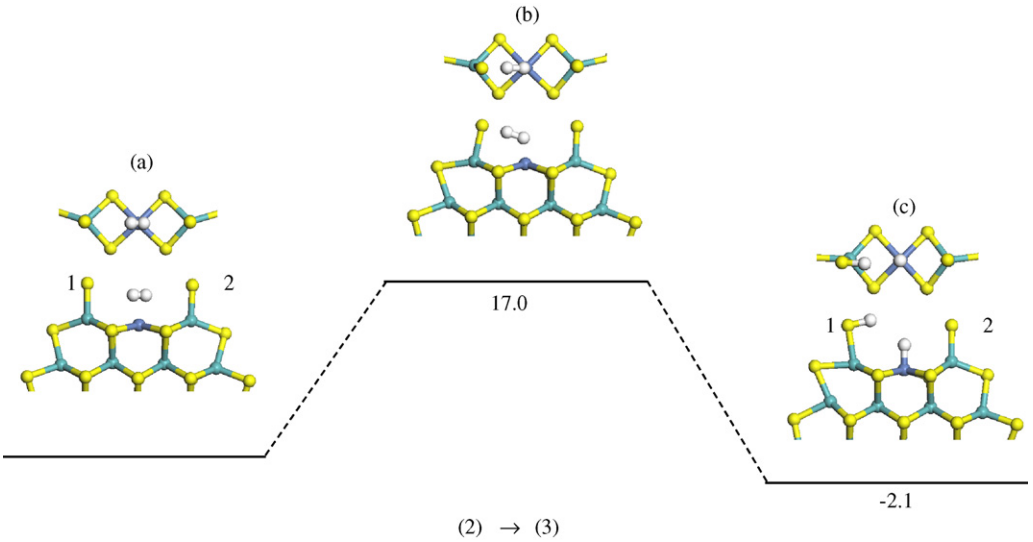

Fig. 4. Dissociation of an H_2 molecule on the surface of the NiMoS cluster yielding an SH and an NiH fragment (step 2 → 3, Fig. 2). The structures in the energy diagrams show side (below) and top views. The full structure of the catalyst particle is shown in Fig. 1e. Energy values of the transition state and the product are relative to that of the educt.

3.2. Adsorption and reaction of DBT to BP

The initial step in this sequence is the adsorption of DBT from the gas phase to a stable equilibrium position above the active site of the NiMoS cluster (Fig. 2, 3 → 4). This process has a very low activation barrier (1.9 kcal/mol) and is exothermic by −10.8 kcal/mol, which reflects the stability of the resulting geometry. In this arrangement (Fig. 5, structure a) the DBT ring is in an upright position above the cluster, but slightly tilted so that the hydrogen functions of the active site point approximately to the C–S bond region. While the structure of the DBT molecule in this position is nearly identical to that of the free molecule, the surface of the cluster shows minor reconstruction. The Mo–S–H fragment has adapted to the presence of the organic molecule by changing the S_1–H distance and the H–S_1–Mo and S_1–Mo–Ni bonding angles (Table 1, column 4). The first step of the desulfurization reaction occurs in a concerted mechanism, which consists of

Table 1
Geometrical parameters of structures in the DBT DDS reaction (Fig. 2)

	1[a]	2[b]	3[c]	4[d]	5[e]	6[f]	7[g]	8[h]	9[i]
d(H–H)		0.76[j]	(2.64)	(2.64)				0.74	
d(Ni–H)		1.85	1.44	1.44					
d(S–H)		(2.88)	1.34	1.35	1.36				1.35[m]
d(Ni–S)					2.25	(2.35)	2.23	2.23[l]	2.31
d(Mo–S_1)	2.13	2.13	2.35	2.34	2.33	2.16	2.33	2.33[l]	2.16
d(Mo–S_2)	2.13	2.14	2.13	2.14	2.13	2.14	2.13	2.13	2.16
d_1(C–S)				1.75[k]					
d_2(C–S)				1.74[k]	1.75				
∠H–S_1–Mo			95.6	97.5	89.6				
∠S_1–Mo–Ni			104.5	105.3	101.8	99.9	82.4	82.2	96.2
∠S_2–Mo–Ni	97.7	96.5	101.8	102.2	96.4	99.6	94.6	94.7	101.4
∠Ni–S–C					113.4				
∠Mo–Ni–Mo	159.2	167.7	165.4	166.8	175.1	171.7	171.6	172.2	170.0

[a] Fig 1e.
[b] Fig. 4a.
[c] Fig. 4c.
[d] Fig. 5a.
[e] Figs. 5c and 6a.
[f] Figs. 6c and 7a.
[g] Fig. 7c.
[h] Fig. 8a.
[i] Fig. 8c.
[j] H_2: *d*(H–H) = 0.73 Å.
[k] DBT: $d_1 = d_2 = 1.74$ Å.
[l] $d(S_{Mo}–S_{Ni}) = 2.07$ Å.
[m] H_2S: *d*(S–H) = 1.33 Å.

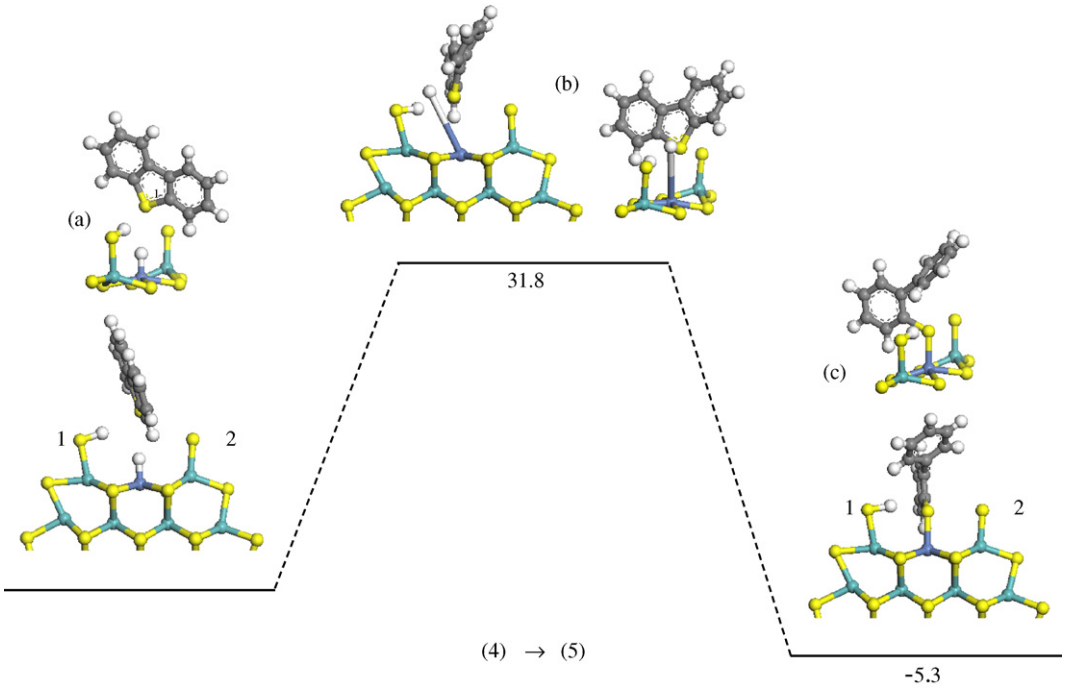

Fig. 5. Adsorption of a DBT molecule on the Ni center of the NiMoS cluster under C–S bond breaking and formation of the BPS intermediate (step 4 → 5, Fig. 2).

three elementary processes: breaking of one C–S bond, H-transfer from the Ni centre to the vacant position of the benzene ring and formation of a BPS–Ni complex. The distance of the resulting Ni–S bond (d(Ni–S) = 2.25 Å) is close to that of a covalent single bond (d_{cov}(Ni–S) = r_{cov}(Ni) + r_{cov}(S) = 1.15 + 1.04 = 2.19 Å). Due to the disappearance of the central five-membered ring of the DBT molecule, the BPS intermediate is not planar but the benzene rings are rotated by 65.8° along the interconnecting C–C bond. This reaction is exothermic by −5.3 kcal/mol, has an activation energy of 31.8 kcal/mol and is the step with the highest barrier in our mechanism. Next the BPSH molecule forms (Fig. 2, 5 → 6) in a slightly exothermic process (ΔH = −4.7 kcal/mol), which has an activation energy of only 9.7 kcal/mol. This rather low activation energy can be explained with the geometry of the BPS intermediate (Fig. 5, structure c). The elementary steps that occur here (Fig. 6, a → c) are the transfer of the H atom of the S–H group to the S atom of the BPS–Ni complex under simultaneous breaking of the Ni–S bond and release of the BPSH molecule. This process involves only a minor redistribution of the H atom between the

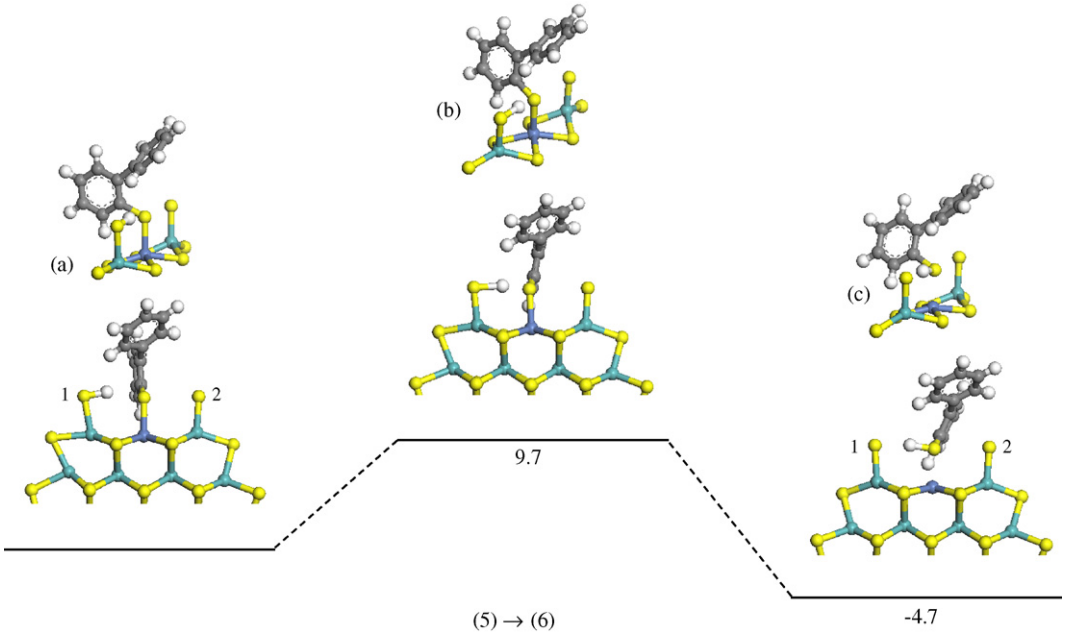

Fig. 6. Formation of BPSH via H-transfer from the catalyst particle (step 5 → 6, Fig. 2).

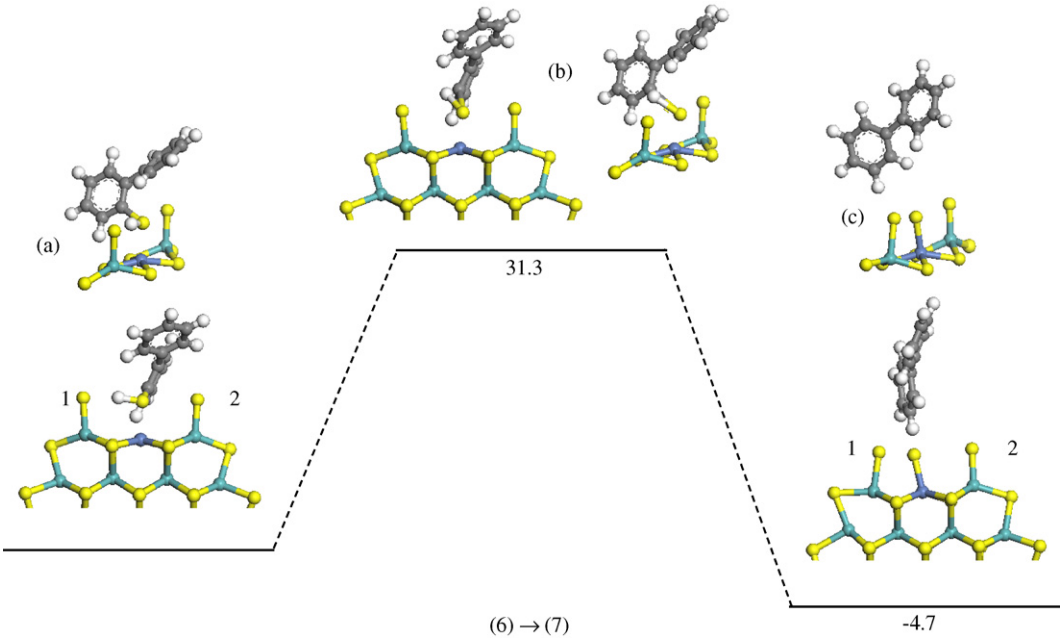

Fig. 7. Formation of BP from BPSH (step 6 → 7, Fig. 2).

two sulfur atoms, as well as a translational movement of the BPSH molecule accompanied by a weak reorientation. The redistribution of the H atom can nicely be seen from the respective S–H distances, which are in the initial state (Fig. 6, structure a): $d(S_1–H) = 1.36$ Å, $d(S_{BPS}–H) = 2.25$ Å, and in the final state (Fig. 6, structure c): $d(S_1–H) = 2.20$ Å, $d(S_{BPS}–H) = 1.36$ Å.

The translational movement and reorientation of the BPSH molecule are reflected in an increase of the Ni–S distance by 0.1 Å and a lowering of the torsion angle from 65.8° to 51.9°. The final step is the formation of the BP molecule and consists essentially in breaking the C–S and SH bonds of the BPSH molecule. While the H atom saturates the aromatic ring, the S atom bonds to the Ni centre. Once the BP molecule is formed, it moves away from the surface and adjusts its geometry (Fig. 7, structure c). Breaking of two bonds, together with a complex movement and reorientation of a large organic molecule, is energetically expensive, and, therefore the calculated activation energy of 31.4 kcal/mol is not surprising. In an alternative pathway we adsorbed the BPSH molecule on a new site with SH and NiH groups (as in Fig. 2, structure 3) and considered a C–S bond breaking mechanism similar to the first hydrogenolysis step. The idea behind this alternative is that the C–S bond in the BPSH molecule is not part of the aromatic ring system as in DBT, which we believed might lead to a lower activation energy for the C–S bond breaking. The calculated activation energy, however, is of the same order (31.3 kcal/mol). In the final state of this reaction step (Fig. 7, structure c) the Ni centre

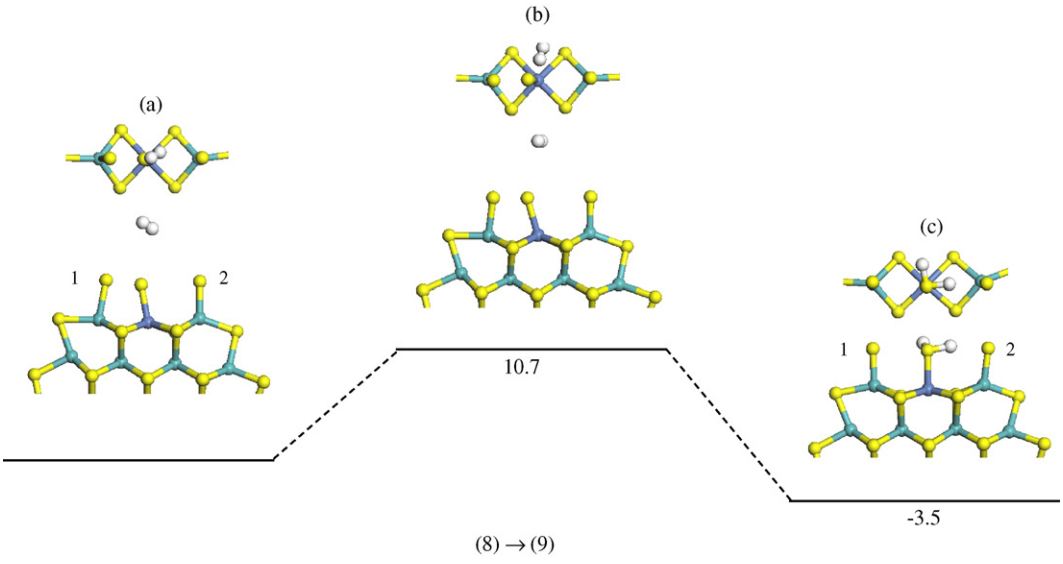

Fig. 8. Cleavage of the catalyst surface through reaction with H_2, during which the Ni–S group reacts to Ni–SH_2 (step 8 → 9, Fig. 2).

is forced into an electronically unfavourable five-fold coordination geometry. The surface adjusts to this situation by coupling the sulfur ligand of the Ni with that of the adjacent Mo centre (S_1). The distance between them is $d(S_1–S_{Ni}) = 2.07$ Å, which means that the bond contains significant π contributions. Thus the surface fragment is in fact an S_2 ligand with two end-on bonded metal centres. This coordination geometry of the S_2^{2-} ligand is not the most common, but there are examples known for certain combinations of transition-metals, among them Mo and Ni [32]. Once the C–S bond of the BPSH molecule is broken and sulfur is substituted by hydrogen, the formed BP molecule moves away from the cluster and adjusts its torsion angle to that of the free molecule (34.5°).

3.3. Cleavage of the catalytic site

The final reaction cascade in our mechanism converts the catalyst particle into its initial state by removing the sulfur from the Ni atom of the cluster. This is done by converting the Ni–S fragment with H_2 into a Ni–SH_2 group and subsequent release of neutral H_2S (Fig. 2, 8 → 9 → 10). In preparation of this reaction cascade the BP molecule must move into the gas phase and an H_2 molecule must be adsorbed at a stable equilibrium position above the active site of the cluster (Fig. 2, 7 → 8), which is the first endothermic step in our mechanism ($\Delta H = 14.1$ kcal/mol). The H_2 molecule finds a position above the Ni–S fragment ($d(S_{Ni}–H) = 3.3$ Å) remaining in its undisturbed state, but interfering with the surface stabilization, which is reflected in a slight increase of the S–S distance to $d(S_{Mo}–S_{Ni}) = 2.09$ Å (Fig. 8, structure a). Moving the H_2 molecule towards the S ligand splits the S_2 couple and weakens the Ni–S interaction: $d(S_{Mo}–S_{Ni})$ increases to 3.21 Å and d(Ni–S) increases from 2.23 to 2.31 Å (Fig. 8, structure c). Finally the H_2S molecule is released into the gas phase, which is endothermic by 6.4 kcal/mol and has a moderate activation energy of 10.8 kcal/mol.

4. Conclusion

The most important results of our DFT calculations can be summarized as follows: our calculated mechanism of the DBT DDS reaction consists of nine individual reaction steps that can be grouped together to three reaction cascades, i.e., the activation of H_2, the reaction of DBT to BP and the cleavage of the catalyst surface. The overall process is exothermic by −11.6 kcal/mol. Most of the reaction steps are exothermic with moderate activation energies around 10 kcal/mol. Four reaction steps have higher activation energies. Two of them involve C–S bond breaking and show similar high activation energies of 31.8 (DBT → BPS) and 31.4 kcal/mol (BPSH → BP). The two others are the heterolytic splitting of H_2 leading to S–H and Ni–H surface groups (17.0 kcal/mol) and the release of the BP molecule from the active site of the catalyst particle (17.1 kcal/mol).

Acknowledgments

We thank Prof. Dr. Roel Prins (ETH Zurich) for valuable discussions. This work was supported by Shell Global Solutions International BV.

References

[1] R. Prins, V.H.J. de Beer, G.A. Somorjai, Catal. Rev.-Sci. Eng. 31 (1989) 1.
[2] H. Topsøe, B.S. Clausen, F.E. Massoth, Hydrotreating Catalysis, Science and Technology, Springer, Berlin, 1996.
[3] M.C. Zonnevylle, R. Hoffmann, Surf. Sci. 199 (1988) 320.
[4] P. Raybaud, J. Hafner, G. Kresse, H. Toulhoat, Phys. Rev. Lett. 80 (1998) 1481.
[5] S. Cristol, J.F. Paul, E. Payen, D. Bougeard, F. Hutschka, J. Hafner, Stud. Surf. Sci. Catal. 128 (1999) 327.
[6] L.S. Byskov, J.K. Nørskov, B.S. Clausen, H. Topsøe, J. Catal. 187 (1999) 109.
[7] L.S. Byskov, J.K. Nørskov, B.S. Clausen, H. Topsøe, Catal. Lett. 64 (2000) 95.
[8] P. Raybaud, J. Hafner, G. Kresse, S. Kasztelan, H. Toulhoat, J. Catal. 189 (2000) 129.
[9] P. Raybaud, J. Hafner, G. Kresse, S. Kasztelan, H. Toulhoat, J. Catal. 190 (2000) 128.
[10] S. Cristol, J.F. Paul, E. Payen, D. Bougeard, S. Clemendot, F. Hutschka, J. Phys. Chem. B 104 (2000) 11220.
[11] S. Cristol, J.F. Paul, E. Payen, D. Bougeard, S. Clemendot, F. Hutschka, J. Phys. Chem. B 106 (2002) 5659.
[12] A. Travert, H. Nakamura, R.A. van Santen, S. Cristol, J.F. Paul, E. Payen, J. Am. Chem. Soc. 124 (2002) 7084.
[13] S. Cristol, J.F. Paul, E. Payen, D. Bougeard, F. Hutschka, S. Clemendot, J. Catal. 224 (2004) 138.
[14] T. Todorova, V. Alexiev, R. Prins, Th. Weber, Phys. Chem. Chem. Phys. 6 (2004) 3023.
[15] M.J. Girgis, B.C. Gates, Ind. Eng. Chem. Res. 30 (1991) 2021.
[16] D.D. Whitehurst, T. Isoda, I. Mochida, Adv. Catal. 42 (1998) 345.
[17] W.D. Jones, L. Dong, J. Am. Chem. Soc. 113 (1991) 559.
[18] W.D. Jones, D.A. Vicic, R.M. Chin, J.H. Roache, A.W. Myers, Polyhedron 16 (1997) 3115.
[19] R.J. Angelici, in: Th. Weber, R. Prins, R.A. van Santen (Eds.), Transition Metal Sulphides, Chemistry and Catalysis, Kluwer Acad. Publ., Dordrecht, 1998, p. 89.
[20] C. Bianchini, A. Meli, in: Th. Weber, R. Prins, R.A. van Santen (Eds.), Transition Metal Sulphides, Chemistry and Catalysis, Kluwer Acad. Publ., Dordrecht, 1998, p. 129.
[21] F. Bataile, J.L. Lemberton, P. Michaud, G. Pérot, M. Vrinat, M. Lemaire, E. Schulz, M. Breysse, S.J. Kasztelan, Catalysis 191 (2000) 409.
[22] R.L. Wilson, C. Kemball, J. Catal. 3 (1964) 426.
[23] T. Todorova, R. Prins, Th. Weber, J. Catal. 236 (2005) 190.
[24] T. Todorova, R. Prins, Th. Weber, J. Catal. 246 (2006) 109.
[25] B. Delley, J. Chem. Phys. 92 (1990) 508;
B. Delley, J. Chem. Phys. 113 (2000) 7756.
[26] J.P. Perdew, K. Burke, Y. Wang, Phys. Rev. B 54 (1996) 16533.
[27] K.D. Bronsema, J.L. de Boer, F. Jellinek, Z. Anorg. Allg. Chem. 540/541 (1986) 15.
[28] N. Govind, M. Petersen, G. Fitzgerald, D. King-Smith, J. Andzelm, Comput. Mater. Sci. 28 (2003) 250.
[29] T.A. Halgren, W.N. Lipscomb, Chem. Phys. Lett. 49 (1977) 225.
[30] T. Todorova, V. Alexiev, Th. Weber, Bull. Sci. Technol. Soc. 26 (2006) 314.
[31] M. Sun, A.E. Nelson, J. Adjaye, Catal. Today 105 (2005) 36.
[32] A. Müller, E. Diemann, in: G.W. Wilkinson, R.D. Gillard, J.A. McCleverty (Eds.), Compr. Coord. Chem., vol. 2, Pergamon Press, Oxford, 1987 (Chapter 16.1).